

# Electroinduced Reductive and Dearomative Alkene-Aldehyde Coupling

Liam J. Franov<sup>†</sup>, Tayla L. Wilsdon<sup>†</sup>, Milena L. Czyz<sup>†</sup>, and Anastasios Polyzos<sup>†§\*</sup>

<sup>†</sup> School of Chemistry, The University of Melbourne, Parkville 3010, Victoria, Australia; <sup>§</sup> CSIRO Manufacturing, Research Way, Clayton VIC 3168, Australia

\*Email: [anastasios.polyzos@unimelb.edu.au](mailto:anastasios.polyzos@unimelb.edu.au)

## Abstract

The direct coupling of alkene feedstocks with aldehydes represents an expedient approach to the generation of new and structurally diverse C(sp<sup>3</sup>)-hybridized alcohols that are primed for elaborated into privileged architectures. Despite their abundance, current disconnection strategies enabling the direct coupling of carbon-carbon  $\pi$ -bonds and aldehydes remain challenging because contemporary methods are often limited by substrate or functional group tolerance, and compatibility in complex molecular environments. Here, we report a coupling between simple alkenes, heteroarenes and unactivated aliphatic aldehydes via an electrochemically induced reductive activation of C–C  $\pi$ -bonds. The cornerstone of this approach is the discovery of a rapid alternating polarity (rAP) electrolysis to access and direct, highly reactive radical anion intermediates derived from conjugated alkenes and heterocyclic compounds. Our developed catalyst-free protocol enables direct access to new, and structurally diverse C(sp<sup>3</sup>)-hybridized alcohol products. This is achieved by the controlled reduction of conjugated alkenes and the C2–C3  $\pi$ -bond in heteroarenes via an unprecedented reductive dearomative functionalization for heterocyclic compounds. Experimental mechanistic studies demonstrate that rAP electrolysis is necessary for the controlled generation of radical anion intermediates and promotes a kinetically biased single-electron reduction of the C–C  $\pi$ -bonds over aldehydes. Overall, this technology provides a versatile approach to the reductive coupling of olefin and heterocycle feedstocks with aliphatic aldehydes, offering straightforward access to diverse C(sp<sup>3</sup>)-rich oxygenated scaffolds.

## Introduction

Aldehydes and alkenes occupy a central role in organic chemistry as abundant, structurally diverse and widely accessible building blocks for chemical synthesis. The versatile reactivity of  $\pi$ -systems in C=C and C=O bonds under both polar and radical reaction manifolds facilitates the generation of new C(sp<sup>3</sup>)-hybridized oxygenated alkyl fragments from C(sp<sup>2</sup>)-rich scaffolds in an atom economical fashion. The Paternò–Büchi reaction instantiates the value of aldehyde and alkene coupling by delivering a straightforward route to diverse and medicinally relevant saturated heterocyclic oxetane architectures via cycloaddition.<sup>1</sup> The generation of architecturally diverse alcohols from direct coupling between alkenes and carbonyls via C–C bond formation has equally garnered considerable attention as they are essential structural motifs in pharmaceutical ingredients,<sup>2</sup> agrochemical products and polymeric materials.<sup>3</sup> In this context, the Prins reaction has been used for the construction of functionalized saturated alcohols present in numerous biologically active compounds and natural products (Figure 1a).<sup>4</sup> Although versatile, tactical deployment of the classical Prins reaction in organic synthesis is often impeded by modest chemoselectivity and substrate compatibility,<sup>5–6</sup> and despite advances in reactions of this type, ample opportunities remain to develop methods enabling the direct coupling of aldehyde and alkene feedstocks via facile C–C bond forming transformations.

Seminal work from Jamison and co-workers<sup>7</sup> leveraging Ni catalysis to furnish allylic and homoallylic alcohols from alkenes and aldehydes represents an important advance in this class of reaction (Figure 1b). Subsequent transition metal-catalyzed methodologies expand its utility toward the generation of saturated aliphatic alcohols; however, the

broad deployment of these synthetic approaches is hampered by undesired aldehyde enolization and the prerequisite for pyrophoric<sup>8</sup> or expensive<sup>9</sup> terminal reductants in superstoichiometric excess. Transfer hydrogenative reductive coupling of activated olefins with aldehydes pioneered by Krische and co-workers<sup>10</sup> represents a notable foray to address these limitations, and substantial progress has been made to engage unactivated olefins.<sup>11</sup> More recently, the development of single-electron reductive activation strategies generate open-shell nucleophilic ketyl radicals from aromatic aldehydes, enabling facile coupling with polarized alkenes. Whilst viable, these photocatalytic approaches

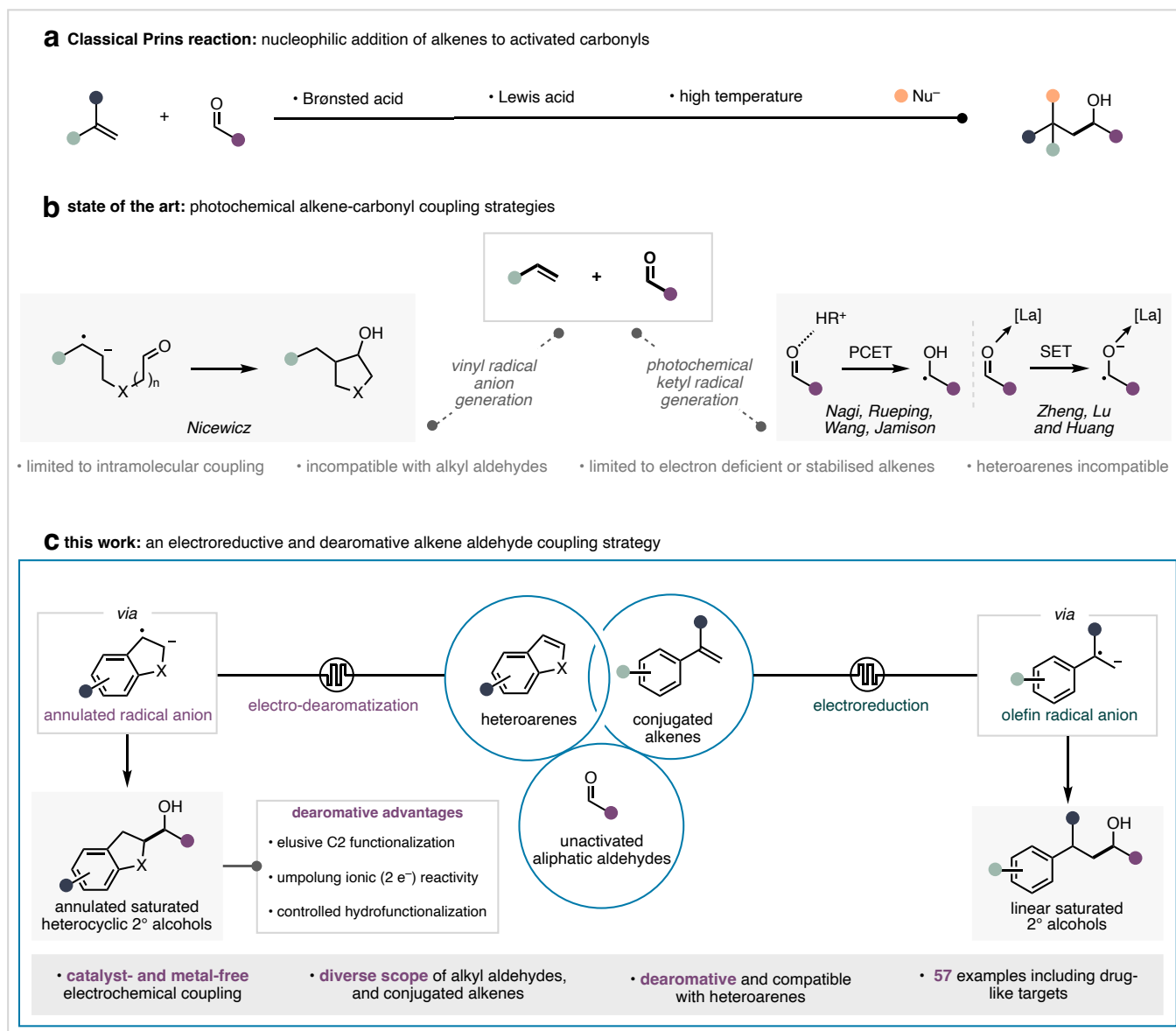


**Figure 1.** Development of an electroreductive and dearomative alkene-aldehyde coupling strategy.

rely on the synergistic use of either proton donors to facilitate proton-coupled electron transfer (PCET),<sup>12</sup> or oxophilic rare earth metals to stabilize the ensuing ketyl radical anion.<sup>13</sup> Furthermore, these protocols are typically incompatible with alkyl aldehydes and necessitate electron-deficient or stabilized alkenes to accommodate philicity matching with the ketyl radical intermediates. As a result, a general reductive alkene-aldehyde coupling strategy remains an unmet challenge in chemical synthesis.

Envisaging a new approach to alkene and aldehyde coupling, we hypothesized that alkene radical anions could be engaged to enhance the weakly nucleophilic character of unactivated  $\pi$ -systems as a general coupling strategy. Under this mechanistic manifold, the activation of alkenes is achieved by direct, one-electron reduction to the

corresponding radical anion, and the enhanced nucleophilicity of alkene radical anions<sup>14</sup> promotes C–C coupling with weakly electrophilic aldehydes without the need for intrinsic or exogenous carbonyl activation. Recently, visible-light photoredox catalysis has been established as a useful tool to generate alkene radical anions from conjugated olefinic substrates.<sup>15</sup> Previous work in our laboratory<sup>16</sup> and pioneering studies by Xiao and Chen<sup>17</sup> have shown that vinyl radical anions are viably furnished by the *in situ* generation of potent photoreductants<sup>18</sup> via photoredox catalysts. This approach to highly reducing photocatalysis overcomes the high onset of reduction for styrenyl substrates ( $E_{red} < -2.5$  V vs SCE),<sup>19</sup> enabling the ensuing vinyl radical anions to undergo intermolecular coupling with superstoichiometric alkyl ketones, while aldehydes were unreactive under these reaction conditions. Seminal studies by Nicewicz<sup>20</sup> demonstrated that highly reducing acridinium<sup>21</sup> photoredox catalysis promoted the intramolecular nucleophilic addition of vinyl radical anions with substrates bearing tethered aldehydes. Although successful, this approach is complicated by the closely matched onset of reduction for aldehydes and unactivated aryl alkenes, engendering unwanted reactivity and decomposition pathways derived from ketyl radical formation. Despite the ongoing progress, a general method enabling coupling of alkene radical anions and aldehydes is beyond the scope of contemporary photoredox approaches.

We therefore questioned if electrochemistry was a viable reactivity platform to achieve alkene-aldehyde coupling via electroreduction of alkenes and the dearomatization of heteroarenes to the corresponding radical anions (Figure 1c). The precise control over the applied potential enables facile reduction of weakly nucleophilic or electrophilic C–C  $\pi$ -bonds into highly nucleophilic radical anion intermediates, without the limitations imposed by photocatalytic systems. Schäfer and co-workers<sup>19c</sup> established that radical anions generated under electrochemical conditions are sufficiently nucleophilic to be trapped by weakly electrophilic solvents, including DMF and CH<sub>3</sub>CN; however, the reaction was complicated by indiscriminate regioselectivity, uncontrollable  $\alpha,\beta$ -bis addition and electrohydrodimerization. We postulated that this promiscuous reactivity is facilitated by the persistent delivery of electrons to the cathode in a direct current setup, coupled with slow mass transfer from the electrode surface.<sup>22</sup> To overcome this issue, we imagined that rapid alternating polarity (rAP) electrolysis, consisting of a millisecond square waveform, could be utilized to circumvent the rapid degradation pathways promoted by direct current electrolysis.

The dimension of electroinduced alkene radical anion and aldehyde coupling could be extended to the C2–C3  $\pi$ -system in heterocyclic feedstocks (Figure 1c). Dearomative reactions of heteroarenes provide an efficient strategy to rapidly access complex, C(sp<sup>3</sup>)-rich heterocyclic architectures from readily accessible planar C(sp<sup>2</sup>) frameworks.<sup>23</sup> Dearomative functionalization reactions provide access to medicinally and biologically relevant three-dimensional heterocyclic scaffolds, whilst simultaneously increasing the molecular complexity in a single unit operation.<sup>24</sup> Single-electron variants typically provide the most efficacious routes and occur via regioselective addition of carbon-centered radicals to C2 of the C2–C3  $\pi$ -system via Giese-type addition. However, these protocols are impeded by the inherent stability of the extended aromatic system and requirement for radical philicity matching.<sup>25</sup> As a result, intramolecular radical addition<sup>26</sup> or pre-activation of the heterocyclic substrate with electron-withdrawing substituents at C3 is often necessary.<sup>27</sup> Recent progress has been made to overcome some of these limitations through the generation of highly energetic alkyl<sup>28</sup> or ketyl radical<sup>29</sup> fragments and the radical anion of carbon dioxide (CO<sub>2</sub><sup>-</sup>)<sup>30</sup> that undergo intermolecular addition to unactivated heterocyclic rings. These transformations successfully deliver new C(sp<sup>3</sup>)-rich centers to heterocyclic scaffolds; however, the necessary generation of high energy radicals and the resultant C2 regioselectivity narrows the range of viable coupling partners and products to Giese-type adducts. By reimagining the C2–C3  $\pi$ -bond of heteroarenes as a radical anion progenitor, new retrosynthetic disconnections to dearomative

transformations can be considered. Consistent with alkene feedstocks, this unprecedented strategy leverages the latent nucleophilicity of radical anions derived from single-electron reduction of the C2–C3  $\pi$ -bond of heteroarenes, enabling C–C bond formation with carbonyl electrophiles. In this light, we expect this approach to unlock a nucleophilic C2 reactivity umpolung for orthogonal heteroarene functionalization with  $2e^-$  electrophiles by leveraging benzylic radical stability at C3, thus permitting new opportunities for the dearomative diversification of heteroarenes with aldehydes to furnish saturated heterocyclic rings bearing secondary alcohol functionality.

Herein, we report a successful electroreductive alkene-aldehyde coupling strategy that harnesses the chemoselective redox environment of rAP to control and direct styrenyl and heteroaryl radical anions toward unactivated, aliphatic aldehydes to furnish new and structurally diverse C(sp<sup>3</sup>)-hybridized alcohols. This approach is catalyst-, metal- and additive-free, and does not require sacrificial electrodes. Moreover, the method exhibits a broad substrate scope, full selectivity for alkene reduction, and is amenable to simple alkene feedstocks and conjugated C–C  $\pi$ -bonds possessing deep reduction potentials ( $E_{red} \geq -3.0$  V vs SCE) without the need for prefunctionalization.

## Results and Discussion

Our proposed design blueprint for the electroreductive alkene-aldehyde coupling reaction is detailed in Figure 2. We immediately anticipated the main challenge of intermolecular electroreductive coupling would arise from controlling fast olefinic overreduction, as well as ensuring full selectivity for reduction of the olefin in the presence of redox-active aldehydes. To this end, alternative waveforms were considered as a useful solution through the establishment of a unique chemoselective environment. In particular, rapid alternating polarity (rAP) electrolysis, consisting of a millisecond square waveform, enables instantaneous electrode polarity inversion in a precisely timed square wave. This generates a distinct redox environment conducive only to reactions whose kinetics surpass the switching frequency of the wave.<sup>31</sup> We envisioned that orchestrating an electrode polarity inversion immediately following cathodic generation of the olefinic radical anion circumvents undesirable overreduction.<sup>32</sup> This strategy permits the spacial and temporal generation of the radical anion intermediate and affords a unique reactivity environment for its interception with an exogenous aldehyde reagent. Unlike most metal-catalyzed approaches, this electroreductive process can occur at room temperature in an operationally simple undivided cell. Moreover, reduction and protonation of the ensuing benzylic radical ameliorates the requirement for additional hydrogen-based reductants in related metal-catalyzed coupling strategies.

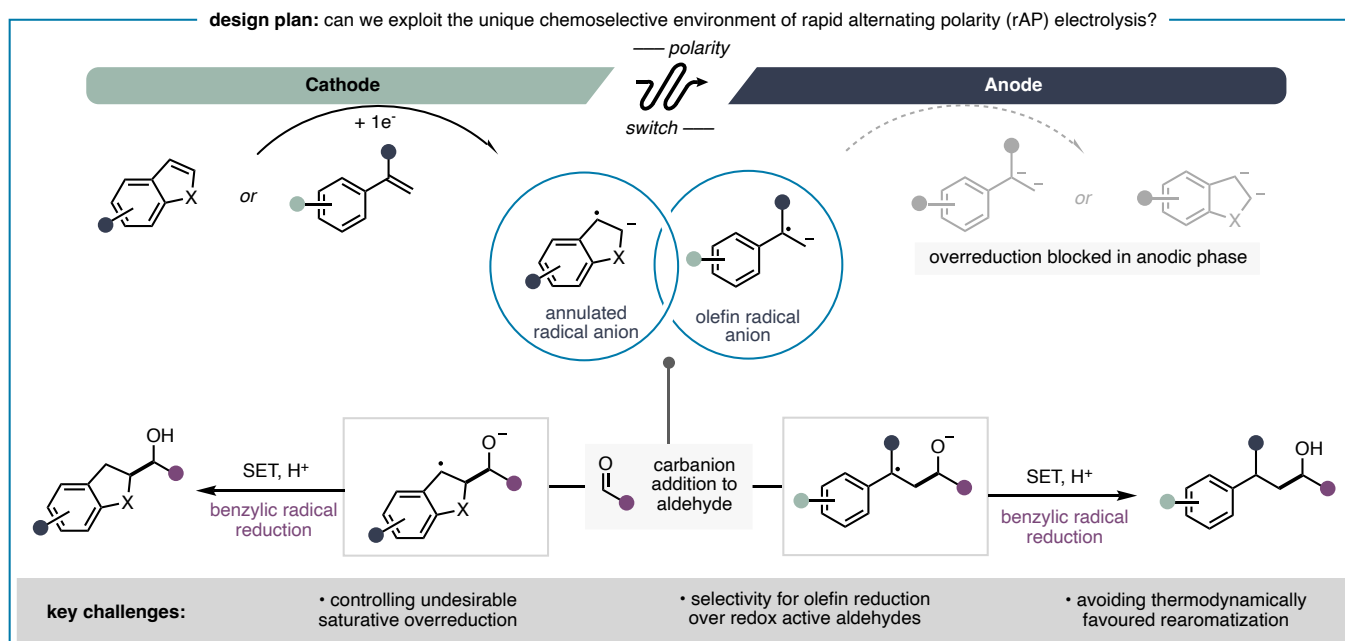
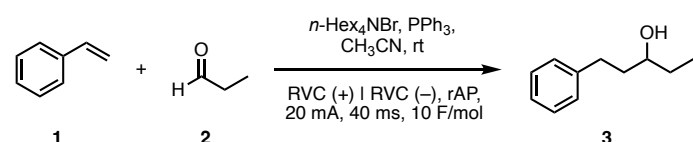


**Figure 2.** Reaction design harnessing rapid alternating polarity electrolysis to circumvent chemoselectivity challenges encountered with direct current waveform.

### Reductive Alkene-Aldehyde Coupling

Investigations were initiated by exploring the direct coupling of styrene (**1**) ( $E_{1/2} = -2.58$  V vs SCE) with propionaldehyde (**2**) ( $-2.45$  V vs SCE). Reaction optimization commenced under rAP electrolysis using reticulated vitreous carbon (RVC) electrodes at constant current (20 mA) in the presence of triphenylphosphine ( $\text{PPh}_3$ ) as a sacrificial electron donor and tetrabutylammonium bromide ( $n\text{-Bu}_4\text{NBr}$ ) as the electrolyte (Table 1).

**Table 1.** Selected optimization and control experiments for rAP-enabled alkene-aldehyde coupling reaction<sup>a</sup>



entry <sup>b</sup>	deviations	yield [%] <sup>c</sup>
1	none	85 <sup>d</sup>
2	no electricity	0
3	DC instead of rAP	14
4	DC instead of rAP, divided cell	0
5	no $\text{PPh}_3$	0
6	10 ms instead of 20 ms	23
7	1 equiv. aldehyde instead of 3 equiv.	38
8	graphite (+/-) instead of RVC (+/-)	0
9	$n\text{-Bu}_4\text{NBr}$ instead of $n\text{-Hex}_4\text{NBr}$	82
10	$n\text{-Et}_4\text{NBr}$ instead of $n\text{-Hex}_4\text{NBr}$	44

<sup>a</sup>For full optimization, see Supporting Information. <sup>b</sup>Reactions were performed on a 0.4 mmol scale with aldehyde (3.0 equiv.), electrolyte (0.2 M), and  $\text{PPh}_3$  (3.0 equiv.) in  $\text{CH}_3\text{CN}$  (0.1 M) at rt, and sparged with  $\text{N}_2$  for 30 s prior to electrolysis. <sup>c</sup>Yield determined by  $^1\text{H}$  NMR spectroscopy using 1,4-dioxane as an internal standard. <sup>d</sup>Isolated yield.

Under a polarity switch frequency of 80 ms, full conversion of starting material was observed with the desired 1-phenylpentanol **3** forming in 32% <sup>1</sup>H NMR yield. It was reasoned that a relatively slow polarity switch may promote competitive over-reductive decomposition of the alkene. Consistent with this logic, a higher frequency polarity switch (40 ms) resulted in a detectable improvement in yield (37%). Frequencies below 40 ms resulted in a reduction in yield, likely due to the operation of a capacitive rather than Faradaic current.<sup>33</sup> Next, variation of aldehyde stoichiometry was examined and three equivalents generated a substantive increase in yield (83%). Further optimization considered the influence of the electrolyte on the reaction. Tetraalkylammonium salts displayed a marked sensitivity of product yield with the counteranion variation. The reaction displayed highest compatibility with bromide (Br<sup>-</sup>) counteranions, and yields diminished substantially with anion variants. Longer chain tetraalkylammonium cations were also effective, with *n*-Hex<sub>4</sub>NBr providing the desired product **3** in 85% isolated yield. The dependence on chain length for tetraalkylammonium cations was evidenced by a slight decrease to 82% yield for *n*-Bu<sub>4</sub>NBr, followed by a substantial decrease to 44% when *n*-Et<sub>4</sub>NBr was employed. In both cases, olefinic overreduction was observed. This observation implies an influence of larger cationic radii imposing a wider inner Helmholtz plane at the electrode surface.<sup>34</sup> We posited this may increase Coulombic repulsion of protons, in addition to weaker ion-pairing interactions to the olefinic radical anion, and the net effect is a further suppression of unwanted olefinic saturative reduction. Our final conditions comprised three equivalents of aldehyde, *n*-Hex<sub>4</sub>NBr at 0.2 M concentration with respect to the solvent, and three equivalents of PPh<sub>3</sub> as a sacrificial electron donor in CH<sub>3</sub>CN at 0.1 M concentration. The reaction deployed RVC as both the working and counter electrode and was undertaken via constant current electrolysis (20 mA) at room temperature with rAP at 40 ms frequency until consumption of 10 F/mol.

With the optimized conditions established, we evaluated the scope of the alkene-aldehyde coupling, first with respect to the vinylarene (Figure 3). The reaction was amenable to both electron-deficient- (**4**) and electron-rich olefins (**5** – **6**), albeit with greater tolerance for the latter. Notably, this electronic bias for electron-rich olefins is in direct contrast to the expected reactivity pattern for aldehydic ketyl radical addition to a neutral olefin, supporting our initial postulate that a ‘radical anion-first’ is the plausible mechanistic pathway. Protodehalogenation was not observed for both chlorine- and fluorine-substituted adducts (**7** – **8**), evidencing chemoselectivity for cathodic reduction of the olefin. Steric congestion on the aromatic ring was well tolerated (**9** – **10**), as well as various heterocyclic derivatives (**11** – **12**). Notably, redox-active sulfur in benzothiophene-derived **13** remained intact, demonstrating favorable reductive selectivity for the exocyclic π-system. The reaction was compatible with α-alkyl substituted vinylarenes containing a range of cyclic and acyclic aliphatic substituents (**14** – **20**), for which the corresponding secondary alcohols were isolated as diastereomeric mixtures. Heteroatoms at this position (**21**) were well tolerated, as was the internal olefin within norbornene-bearing **22**.

We next evaluated the scope of aliphatic aldehydes. Cyclic (**23** – **27**) and acyclic variants (**28**– **33**), as well as nitrogen- and oxygen-containing heterocycles and carbocycles (**34** – **37**), proceeded in good to excellent yields. Significantly, the reaction was compatible with enolizable aldehydes, showcasing the selectively nucleophilic nature of the alkene radical anion. The reaction was remarkably efficient even in the presence of a sterically congested α-quaternary center (**33**), and the absence of any Giese addition of a *t*-Bu radical (generated via α-scission of a pivaldehyde-derived ketyl radical)<sup>12a</sup> further evidenced an olefinic radical anion pathway. Moreover, competitive reduction of the isoprenyl group was not observed for citronellal-derived **39**. For highly polar substrates where chromatographic isolation proved challenging in the presence of triphenylphosphine oxide, replacement of PPh<sub>3</sub> with

phosphite esters such as  $P(i\text{-PrO})_3$  allowed straightforward product isolation with negligible erosion of yields (see Supporting Information). Importantly, acetaldehyde-derived **28** bears close resemblance to rhododendrol, and its butan-2-ol scaffold is found in several natural products and pharmaceutically relevant targets, as well as being a useful handle for late-stage synthetic manipulations.<sup>35</sup>

Secondary alcohols are ubiquitous motifs in natural products and small molecule therapeutics. To establish the versatility of our developed methodology, we synthesized antitrypanosomal candidate<sup>36</sup> **40** and acetylcholinesterase inhibitor<sup>37</sup> **41** each in one step from commercially available precursors (Figure 4a). We next sought to showcase the synthetic utility of the reaction product by leveraging the secondary alcohol motif as a handle for synthetic manipulation. We elected alcohol **28** as an exemplar partner by virtue of its medicinally relevant methyl terminus. Classical Koenigs–Knorr glycosylation of alcohol **28** delivered rhododendrin analogue **42** in 42% yield. In recent years, numerous deoxygenative cross-coupling strategies have been disclosed to forge C–C bonds between alcohols and various coupling partners.<sup>38</sup> Employing technology developed by MacMillan and co-workers, we effected the deoxygenative alkylation<sup>38g</sup> and arylation<sup>38a</sup> of alcohol **28** via exchange of the hydroxy group with a heterocyclic azetidine fragment and a quinoline motif, respectively, to furnish **43** and **44**. Together with **42**, these examples illustrate that, in only two steps, a substantive increase in molecular complexity is realized from simple commercial building blocks.

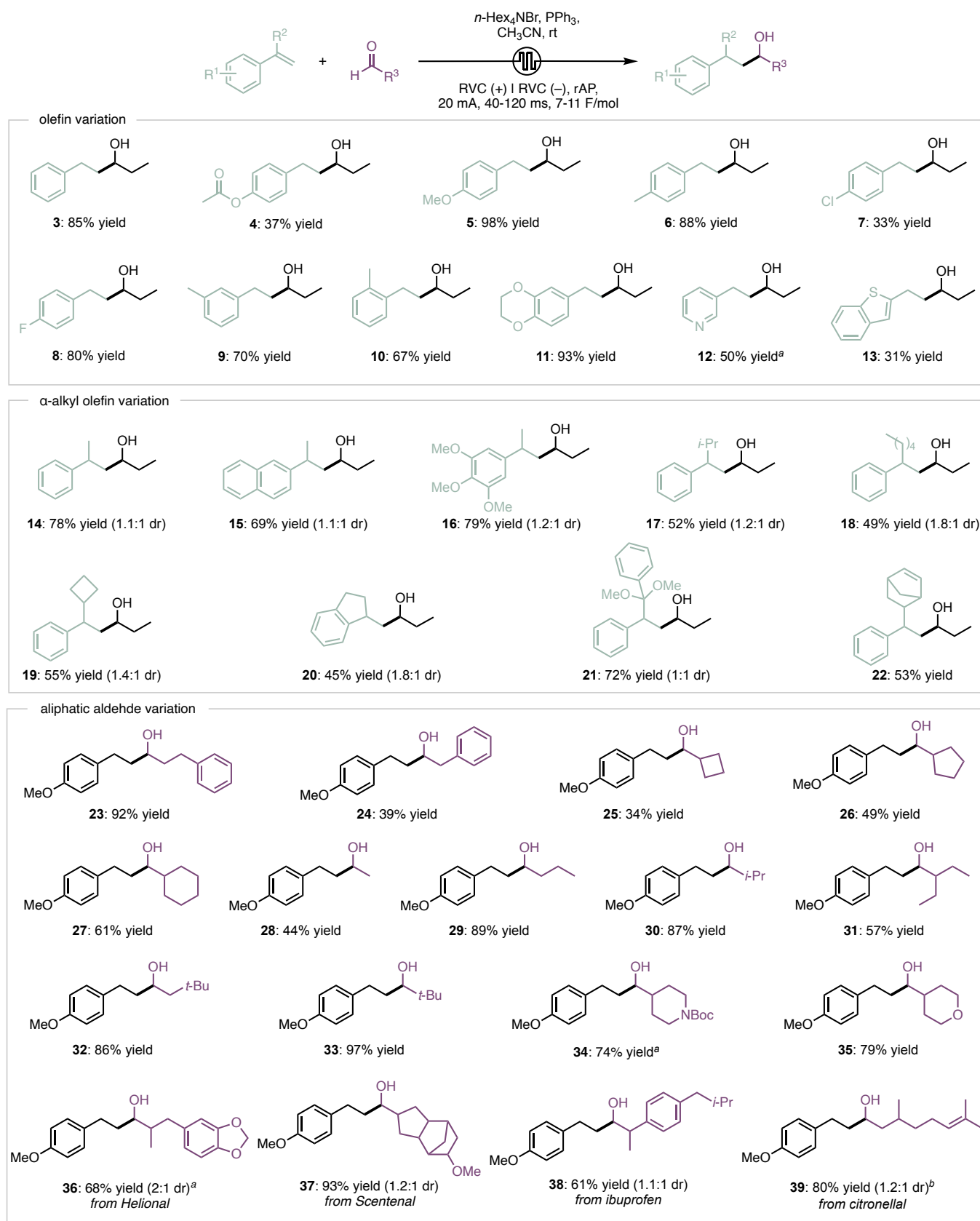


**Figure 3.** Scope of rAP-enabled alkene-aldehyde coupling. Reactions were performed on a 0.4 mmol scale with aldehyde (3.0 equiv.), *n*-Hex<sub>4</sub>NBr (0.2 M), and PPh<sub>3</sub> (3.0 equiv.) in CH<sub>3</sub>CN (0.1 M) at rt, and sparged with N<sub>2</sub> for 30 s prior to electrolysis. All yields are isolated. Diastereomeric ratios are ascribed with respect to the crude material unless otherwise noted. <sup>a</sup>P(*i*-PrO)<sub>3</sub> (3.0 equiv) used instead of PPh<sub>3</sub>. <sup>b</sup>Diastereomeric ratio ascribed with respect to the purified material.



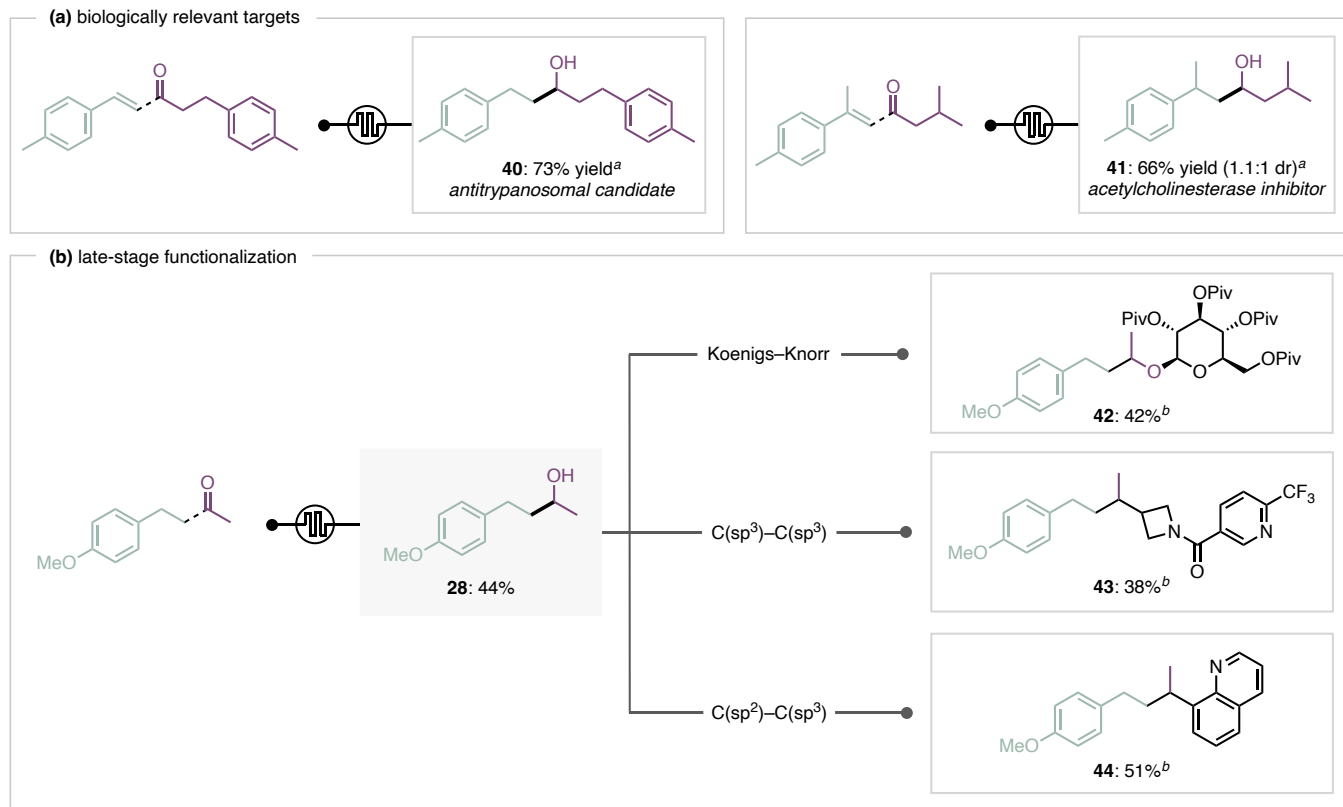


**Figure 4.** Synthetic applications of electroreductive alkene-aldehyde coupling; (a) synthesis of biologically relevant targets; (b) late-stage functionalization of secondary alcohol products. All yields are isolated. <sup>a</sup>Reaction was performed on a 0.4 mmol scale with aldehyde (3.0 equiv.), *n*-Hex<sub>4</sub>NBr (0.2 M), and PPh<sub>3</sub> (3.0 equiv.) in CH<sub>3</sub>CN (0.1 M) at rt, and sparged with N<sub>2</sub> for 30 s prior to electrolysis. <sup>b</sup>See supporting information for detailed reaction conditions.

### Dearomative Heteroarene-Aldehyde Coupling

Encouraged by the remarkable compatibility with vinylarenes, we imagined this protocol could be extended to heteroaryl systems. Specifically, we identified abundant feedstock heteroarenes such as benzofurans and benzothiophenes, wherein the C2–C3  $\pi$ -bond serves as a latent handle for the introduction of higher-order C-sp<sup>3</sup> hybridized carbon centers via dearomative hydrofunctionalization.<sup>29</sup> We therefore questioned whether electroreduction of these structural motifs would uncover the latent reactivity of heteroaryl C2–C3 radical anions for subsequent trapping with aliphatic aldehydes. Gratifyingly, exposure of various heteroaryl scaffolds to slightly modified rAP conditions (see Supporting Information) in the presence of unactivated aliphatic aldehydes furnished the desired 2-substituted products in moderate to good yields (Figure 5). Indeed, to the best of our knowledge, this constitutes the first example of intermolecular, dearomative 2-functionalization of heteroarenes via reductive activation of the heteroarene. We were pleased to observe that both benzofuran (**45** – **49**) and benzothiophene (**50** – **54**) scaffolds were amenable to the reaction conditions. Various alkyl (**46**, **51**) and aryl (**47**, **52**) substituents located at C3 and C5 were tolerated, and the reaction profile exhibited a similar electronic bias toward electron-rich heteroarenes (**48** – **49**, **53** – **54**). Protodehalogenation was not observed for fluorine-containing heteroarenes (**54** – **59**), demonstrating favorable chemoselectivity for cathodic reduction of the C2–C3  $\pi$ -system. The reaction was compatible with aldehydes bearing cyclic and acyclic alkyl substitution (**55** – **58**), as well as the pharmacophoric tetrahydropyran scaffold (**59**). We anticipate that these discoveries will give new impetus to harness the reactivity umpolung of heteroaryl radical anions for dearomative functionalization.

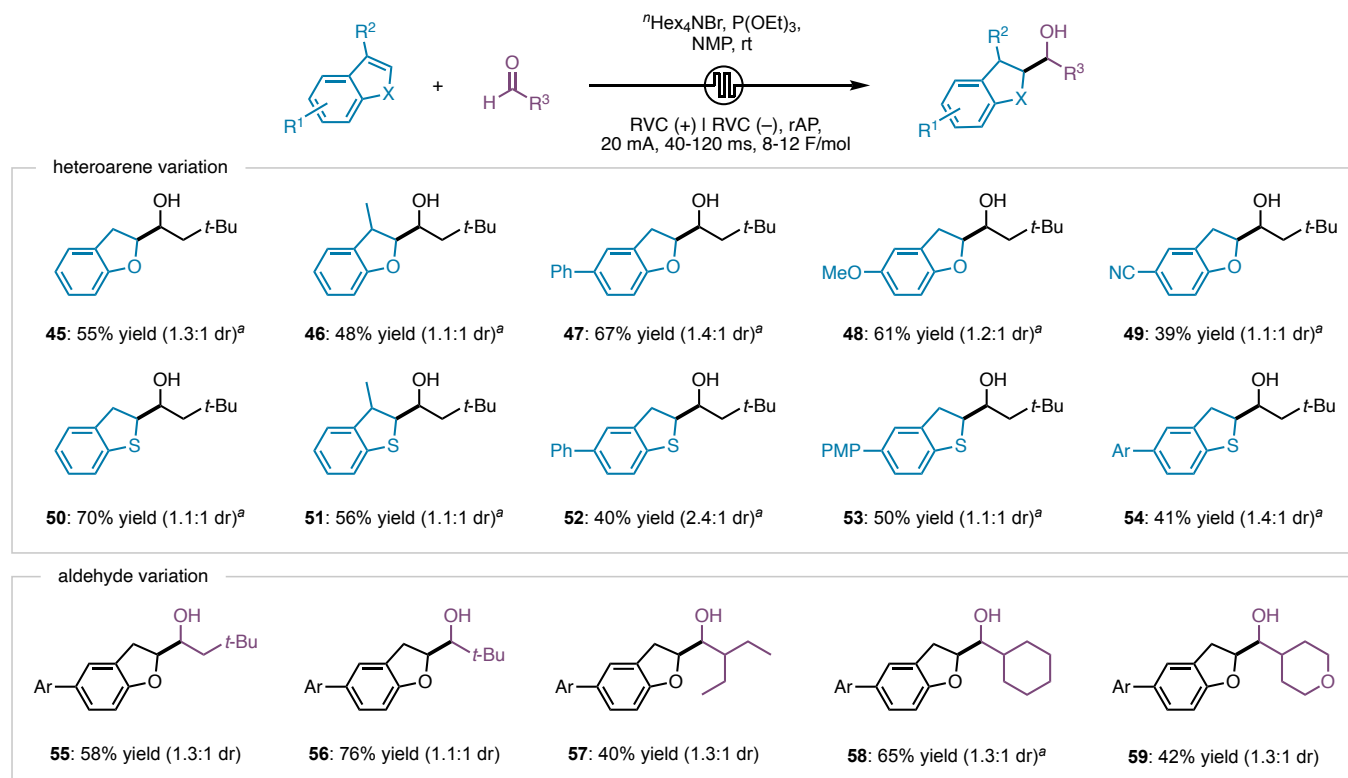


**Figure 5.** Scope of rAP-enabled hetero(arene)–aldehyde coupling. <sup>b</sup>Reactions were performed on a 0.4 mmol scale with aldehyde (3.0 equiv.), *n*-Hex<sub>4</sub>NBr (0.2 M), and P(OEt)<sub>3</sub> (3.0 equiv.) in 1-methyl-2-pyrrolidinone (NMP) (0.1 M) at rt, and sparged with N<sub>2</sub> for 30 s prior to electrolysis. Ar = (4-fluorophenyl). All yields are isolated. Diastereomeric ratios are ascribed with respect to the crude material. <sup>a</sup>Diastereomeric ratio ascribed with respect to the purified material.

## Mechanistic Studies

Having established a broad scope for the alkene–aldehyde coupling and an unprecedented dearomative variant, attention was focused on probing the mechanism of this reaction. These studies focused on vinylarene–aldehyde coupling as a representative transformation. We recognized that unactivated vinylarenes and aliphatic aldehydes possess thermodynamically competitive reduction potentials. Indeed, linear sweep voltammograms (LSVs) recorded for styrene (**1**) (Figure 5ei, purple trace) and propionaldehyde (**2**) (Figure 5ei, green trace) under experimentally relevant conditions, revealed discernible anodic onset potential of propionaldehyde (**2**) compared to styrene (**1**). It was reasoned that application of an overpotential to a mixture of (**1**) and (**2**) bearing closely matched onset potentials may lead to product generation via cathodic reduction of either the olefin or the aldehyde component.<sup>39</sup> Previously reported electrochemical olefin–carbonyl protocols operating via carbonyl reduction have incorporated specific design elements to facilitate this ‘carbonyl first’ process, such as strong adsorption of a ketyl radical to the electrode surface,<sup>40</sup> or by a PCET mechanism.<sup>12e</sup> We reasoned that similar phenomena may have been operative under our optimized reaction conditions. To elucidate the most dominant operative mechanism, a series of experimental and voltammetric studies were conducted. Subjecting 4-vinylanisole (**60**) to standard rAP conditions for vinylarene coupling in the absence of aldehyde resulted in 61% reduction to corresponding arylalkane **61** (Figure 5ai), supporting a dominant cathodic response of the olefin component in this reaction. In contrast, reaction of cyclohexanecarboxaldehyde (**62**) under equivalent conditions and in the absence of olefin afforded only trace amounts of reduced alcohol **63**, with no pinacol coupling detected. This chemoselective bias was also observed for heteroarenes, with 32% reduction of 5-methoxybenzofuran (**64**) to dihydrobenzofuran **65** under standard rAP

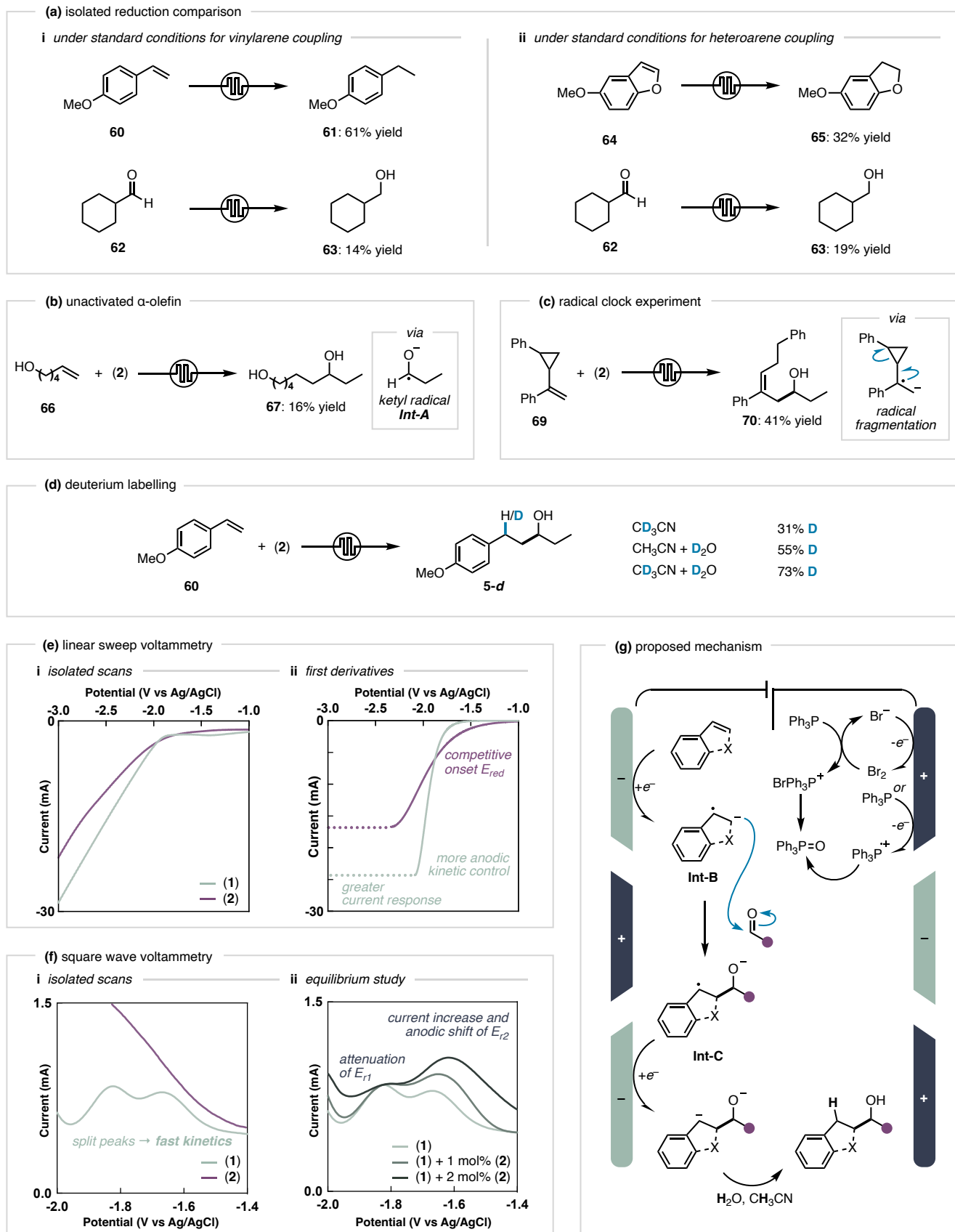


**Figure 5:** Preliminary mechanistic considerations; (a) control experiment: isolated reduction of alkene and aldehyde components under standard conditions for (i) vinylarene coupling and (ii) heteroarene coupling; (b) control experiment: direct reduction of the aldehyde and subsequent addition to an unactivated  $\alpha$ -olefin; (d) radical clock experiment providing evidence for the formation of a benzylic radical intermediate; (e) deuterium-labeling experiments; (f) linear sweep voltammetry: (i) linear sweep voltammograms, (ii) first-derivative of LSVs; (g) square wave voltammetry: (i) square wave voltammograms, (ii) square wave equilibrium study; (g) proposed mechanism.

conditions for heteroarene coupling, compared to 19% reduction of cyclohexanecarboxylaldehyde (**62**) under equivalent conditions. Furthermore, reaction between propionaldehyde (**2**) and redox inactive unactivated  $\alpha$ -olefin **66**, for which addition would have exclusively occurred via ketyl radical **Int-A** (Figure 5c),<sup>40</sup> afforded only trace alcohol **67**. Taken together, these results were consistent with a mechanism involving chemoselective reduction of the alkene to the corresponding nucleophilic olefinic radical anion as the initial step.

Given the discrepancy between the experimental results and the thermodynamic propensity for aldehyde reduction, we questioned if a kinetically biased olefinic reduction was operable under the reactions conditions. To investigate this possibility, we analyzed the shape of the linear sweep voltammetry (LSV) traces recorded for styrene (**1**) and propionaldehyde (**2**) (Figure 5ei). The rate of heterogeneous electron transfer is directly correlated to the magnitude of the current as a function of applied potential.<sup>41</sup> Examining the LSV traces, a rapid kinetic response was observed for (**1**) and exhibited a greater current response throughout the applied overpotential. A similar trend was observed between 5-methoxybenzofuran (**64**) and 3,3-dimethylbutyraldehyde (**68**) (see Supporting Information). We posited that these defining characteristics, which were readily observable in the first derivative of the LSV traces (Figure 5eii), may be attributed to  $\pi$ -stacking interactions between vinylarenes or heteroarenes and the  $sp^2$ -hybridized fullerene structure of RVC,<sup>42</sup> thereby facilitating a kinetically favored heterogeneous electron transfer.

Next, square wave voltammetry (SWV) was performed to provide further insight into the single-electron transfer steps operative at the cathode. This was undertaken through analysis of the shape and position of the SW responses. Styrene (**1**) displayed two resolvable peaks corresponding to the components of an overall reversible, two-electron transfer.<sup>43</sup> In concordance with the onset potential in the LSV, we ascribed the more cathodic peak to  $S \rightleftharpoons S^{\cdot-}$  and the more anodic one to  $S^{\cdot-} \rightleftharpoons S^{2\cdot-}$ . This phenomenon is only observed when electron transfer is very fast.<sup>44</sup> Addition of substoichiometric aliquots of propionaldehyde (**2**) to styrene (**1**) resulted in almost complete attenuation in  $S \rightleftharpoons S^{\cdot-}$  along with a concomitant anodic shift and current increase of  $S^{\cdot-} \rightleftharpoons S^{2\cdot-}$ . This disturbance of the hypersensitive equilibrium between S,  $S^{\cdot-}$  and  $S^{2\cdot-}$  was attributed to the interception of  $S^{\cdot-}$  with neutral propionaldehyde, a pathway that acted as a thermodynamic sink.<sup>44c</sup> It may also provide evidence for an ECEC-type mechanism (each reduction directly followed by a chemical reaction) rather than an EECC-type mechanism (two consecutive reductions followed by two consecutive chemical reactions). Under equivalent SW conditions, propionaldehyde (**2**) did not display resolvable peaks, indicative of rapid decompositional pathways following ketyl radical generation. Taken as a whole, these results are in agreement with a mechanistic pathway involving the kinetically biased cathodic generation of the nucleophilic olefinic radical anion under the rAP reaction conditions.

With these insights in hand, we sought to ascertain whether radical or polar addition of the olefinic radical anion to the aldehyde predominated. Despite delocalization of the additional electron into the surrounding  $\pi$ -framework, recent work by Xiao and Chen<sup>45</sup> as well as in our laboratory<sup>46</sup> has revealed the experimentally distonic-like character of these highly energetic intermediates, with carbanion and radical spin density discretely positioned across the vinyl motif. In light of this, reaction of phenylcyclopropyl olefin **69** under the rAP conditions in the presence of propionaldehyde (**2**) resulted in exclusive formation of ring-opened alcohol **70**. This indicated predominantly radical character at the benzylic position, consistent with polar addition to propionaldehyde (**2**) as the prevailing mechanistic mode. Finally, deuterium labeling studies showed deuterium incorporation at the benzylic position from both  $CD_3CN$  and exogenous  $D_2O$ . Taken with the radical clock experiment, we proposed quenching of the benzylic radical via cathodic radical polar crossover, followed by rapid protonation by solvent or adventitious water. On the basis of these

mechanistic insights, we assigned the major mechanistic pathway of the alkene-aldehyde coupling reaction to the cathodic reduction of the alkene ( $E_1$ ) to corresponding radical anion **Int-B**. Given the dependence of both  $\text{Br}^-$  and  $\text{PPh}_3$ , we speculated a synergistic oxidative relay process whereby  $\text{PPh}_3$  would recycle oxidized  $\text{Br}^-$  to facilitate efficient electron flow. A subsequent electrode polarity switch enabled polar addition of **Int-B** to the aldehyde ( $C_1$ ) to generate distal radical anion **Int-C**, which, after a second electrode polarity switch, underwent cathodic radical polar crossover ( $E_2$ ) and protonation by solvent or adventitious water ( $C_2$ ) to afford the corresponding secondary alcohol.

## Conclusion

In summary, we have disclosed an electroreductive intermolecular coupling reaction between unactivated aryl alkenes or fused ring heterocycles and aliphatic aldehydes. This operationally simple reaction manifold leverages the unique redox environment of rAP electrolysis to access and direct highly reactive radical anion intermediates electrogenerated from the vinyl  $\pi$ -bond in conjugated alkenes and the C2–C3  $\pi$ -bond in heterocycles. We found this catalyst-free protocol avoids uncontrollable  $\pi$ -bond overreduction typically encountered under direct current waveform, giving access to new and structurally diverse  $\text{C}(\text{sp}^3)$ -hybridized alcohols. A salient feature of this method is the unprecedented reductive dearomative functionalization of heteroarenes that leverages the latent reactivity of annulated heteroaryl C2–C3 radical anions for subsequent trapping with aliphatic aldehydes. Critically, we expect this strategy to unlock a nucleophilic C2 reactivity umpolung for orthogonal heteroarene functionalization with  $2e^-$  electrophiles, permitting new opportunities for the regioselective diversification of heteroarenes with a broad range of feedstock electrophiles. Mechanistic studies reveal a kinetically biased single-electron reduction of the vinyl  $\pi$ -bond in conjugated alkenes, and the C2–C3  $\pi$ -bond in heterocycles, to controllably generate the radical anion intermediates, and the chemoselective redox environment of rAP is critical to this chemoselectivity. We believe that the generality and operational simplicity of this transformation provides a viable approach to the reductive coupling of olefins and heterocycles with aliphatic aldehydes, enabling expedient access to  $\text{C}(\text{sp}^3)$ -rich secondary alcohols primed for diversification in chemical research programs across academia and industry.

## References

- (1) Fréneau, M.; Hoffmann, N. The Paternò-Büchi reaction—Mechanisms and application to organic synthesis. *Journal of Photochemistry and Photobiology C: Photochemistry Reviews* **2017**, *33*, 83-108.
- (2) Cramer, J.; Sager, C. P.; Ernst, B. Hydroxyl Groups in Synthetic and Natural-Product-Derived Therapeutics: A Perspective on a Common Functional Group. *J. Med. Chem.* **2019**, *62*, 8915-8930.
- (3) Aziz, S. B.; Brza, M. A.; Nofal, M. M.; Abdulwahid, R. T.; Hussen, S. A.; Hussein, A. M.; Karim, W. O. A Comprehensive Review on Optical Properties of Polymer Electrolytes and Composites. *Materials* **2020**, *13*, 3675.
- (4) (a) Franov, L. J.; Hart, J. D.; Pullella, G. A.; Sumbly, C. J.; George, J. H. Bioinspired Total Synthesis of Erectones A and B, and the Revised Structure of Hyperelodione D. *Angew. Chem. Int. Ed.* **2022**, *61*, e202200420. (b) Han, X.; Peh, G.; Floreancig, P. E. Prins-Type Cyclization Reactions in Natural Product Synthesis. *Eur. J. Org. Chem.* **2013**, *2013*, 1193-1208. (c) Padmaja, P.; Reddy, P. N.; Subba Reddy, B. V. Tandem Prins cyclizations for the construction of oxygen containing heterocycles. *Org. Biomol. Chem.* **2020**, *18*, 7514-7532.
- (5) (a) Blanco-Ania, D.; Rutjes, F. P. J. T. Carbonylonium ions: the onium ions of the carbonyl group. *Beilstein J. Org. Chem.* **2018**, *14*, 2568-2571. (b) Reyes, E.; Prieto, L.; Uria, U.; Carrillo, L.; Vicario, J. L. Recent Advances in the Prins Reaction. *ACS Omega* **2022**, *7*, 31621-31627.
- (6) Ng, S.-S.; Ho, C.-Y.; Schleicher, K. D.; Jamison, T. F. Nickel-catalyzed coupling reactions of alkenes. *Pure Appl. Chem.* **2008**, *80*, 929-939.
- (7) (a) Ng, S.-S.; Jamison, T. F. Simple Alkenes as Substitutes for Organometallic Reagents: Nickel-Catalyzed, Intermolecular Coupling of Aldehydes, Silyl Triflates, and Alpha Olefins. *J. Am. Chem. Soc.* **2005**, *127*, 14194-14195. (b) Ho, C.-Y.; Ng, S.-S.; Jamison, T. F. Nickel-Catalyzed, Carbonyl-Ene-Type Reactions: Selective for Alpha Olefins and More Efficient with Electron-Rich Aldehydes. *J. Am. Chem. Soc.* **2006**, *128*, 5362-5363. (c) Ng, S.-S.; Ho, C.-Y.; Jamison, T. F. Nickel-Catalyzed Coupling of Alkenes, Aldehydes, and Silyl Triflates. *J. Am. Chem. Soc.* **2006**, *128*, 11513-11528.
- (8) (a) Montgomery, J. Nickel-Catalyzed Cyclizations, Couplings, and Cycloadditions Involving Three Reactive Components. *Acc. Chem. Res.* **2000**, *33*, 467-473. (b) Miller, K. M.; Huang, W.-S.; Jamison, T. F. Catalytic

Asymmetric Reductive Coupling of Alkynes and Aldehydes: Enantioselective Synthesis of Allylic Alcohols and  $\alpha$ -Hydroxy Ketones. *J. Am. Chem. Soc.* **2003**, *125*, 3442-3443. (c) Molinaro, C.; Jamison, T. F. Nickel-Catalyzed Reductive Coupling of Alkynes and Epoxides. *J. Am. Chem. Soc.* **2003**, *125*, 8076-8077.

(9) (a) Mahandru, G. M.; Liu, G.; Montgomery, J. Ligand-Dependent Scope and Divergent Mechanistic Behavior in Nickel-Catalyzed Reductive Couplings of Aldehydes and Alkynes. *J. Am. Chem. Soc.* **2004**, *126*, 3698-3699. (b) Chaulagain, M. R.; Sormunen, G. J.; Montgomery, J. New N-Heterocyclic Carbene Ligand and Its Application in Asymmetric Nickel-Catalyzed Aldehyde/Alkyne Reductive Couplings. *J. Am. Chem. Soc.* **2007**, *129*, 9568-9569.

(10) (a) Bower, J. F.; Skucas, E.; Patman, R. L.; Krische, M. J. Catalytic C–C Coupling via Transfer Hydrogenation: Reverse Prenylation, Crotylation, and Allylation from the Alcohol or Aldehyde Oxidation Level. *J. Am. Chem. Soc.* **2007**, *129*, 15134-15135. (b) Hassan, A.; Zbieg, J. R.; Krische, M. J. Enantioselective Iridium-Catalyzed Vinylogous Reformatsky-Aldol Reaction from the Alcohol Oxidation Level: Linear Regioselectivity by Way of Carbon-Bound Enolates. *Angew. Chem. Int. Ed.* **2011**, *50*, 3493-3496. (c) Patman, R. L.; Williams, V. M.; Bower, J. F.; Krische, M. J. Carbonyl Propargylation from the Alcohol or Aldehyde Oxidation Level Employing 1,3-Enynes as Surrogates to Preformed Allenylmetal Reagents: A Ruthenium-Catalyzed C–C Bond-Forming Transfer Hydrogenation. *Angew. Chem. Int. Ed.* **2008**, *47*, 5220-5223. (d) Chen, T.-Y.; Tsutsumi, R.; Montgomery, T. P.; Volchkov, I.; Krische, M. J. Ruthenium-Catalyzed C–C Coupling of Amino Alcohols with Dienes via Transfer Hydrogenation: Redox-Triggered Imine Addition and Related Hydroaminoalkylations. *J. Am. Chem. Soc.* **2015**, *137*, 1798-1801. (e) Kim, I. S.; Ngai, M.-Y.; Krische, M. J. Enantioselective Iridium-Catalyzed Carbonyl Allylation from the Alcohol or Aldehyde Oxidation Level Using Allyl Acetate as an Allyl Metal Surrogate. *J. Am. Chem. Soc.* **2008**, *130*, 6340-6341.

(11) (a) Hong, Y.-T.; Barchuk, A.; Krische, M. J. Branch-Selective Intermolecular Hydroacylation: Hydrogen-Mediated Coupling of Anhydrides to Styrenes and Activated Olefins. *Angew. Chem. Int. Ed.* **2006**, *45*, 6885-6888. (b) Yamaguchi, E.; Mowat, J.; Luong, T.; Krische, M. J. Regio- and Diastereoselective C–C Coupling of  $\alpha$ -Olefins and Styrenes to 3-Hydroxy-2-oxindoles by Ru-Catalyzed Hydrohydroxyalkylation. *Angew. Chem. Int. Ed.* **2013**, *52*, 8428-8431. (c) Xiao, H.; Wang, G.; Krische, M. J. Regioselective Hydrohydroxyalkylation of Styrene with Primary Alcohols or Aldehydes via Ruthenium-Catalyzed C–C Bond Forming Transfer Hydrogenation. *Angew. Chem. Int. Ed.* **2016**, *55*, 16119-16122.

(12) (a) Dong, J.; Wang, Z.; Wang, X.; Song, H.; Liu, Y.; Wang, Q. Ketones and aldehydes as alkyl radical equivalents for C–H functionalization of heteroarenes. *Sci. Adv.* **2019**, *5*, eaax9955. (b) Lee, K. N.; Lei, Z.; Ngai, M.-Y.  $\beta$ -Selective Reductive Coupling of Alkenylpyridines with Aldehydes and Imines via Synergistic Lewis Acid/Photoredox Catalysis. *J. Am. Chem. Soc.* **2017**, *139*, 5003-5006. (c) Fava, E.; Nakajima, M.; Nguyen, A. L. P.; Rueping, M. Photoredox-Catalyzed Ketyl–Olefin Coupling for the Synthesis of Substituted Chromanols. *J. Org. Chem.* **2016**, *81*, 6959-6964. (d) Xia, Q.; Tian, H.; Dong, J.; Qu, Y.; Li, L.; Song, H.; Liu, Y.; Wang, Q. N-Arylamines Coupled with Aldehydes, Ketones, and Imines by Means of Photocatalytic Proton-Coupled Electron Transfer. *Chem. Eur. J.* **2018**, *24*, 9269-9273. (e) Seo, H.; Jamison, T. F. Catalytic Generation and Use of Ketyl Radical from Unactivated Aliphatic Carbonyl Compounds. *Org. Lett.* **2019**, *21*, 10159–10163.

(13) Ye, C.-X.; Melcamu, Y. Y.; Li, H.-H.; Cheng, J.-T.; Zhang, T.-T.; Ruan, Y.-P.; Zheng, X.; Lu, X.; Huang, P.-Q. Dual catalysis for enantioselective convergent synthesis of enantiopure vicinal amino alcohols. *Nat. Commun.* **2018**, *9*, 410.

(14) (a) Mayr, H.; Patz, M. Scales of Nucleophilicity and Electrophilicity: A System for Ordering Polar Organic and Organometallic Reactions. *Angew. Chem., Int. Ed. Engl.* **1994**, *33*, 938-957. (b) Corral-Bautista, F.; Klier, L.; Knochel, P.; Mayr, H. From Carbanions to Organometallic Compounds: Quantification of Metal Ion Effects on Nucleophilic Reactivities. *Angew. Chem. Int. Ed.* **2015**, *54*, 12497-12500.

(15) (a) Du, J.; Espelt, L. R.; Guzei, I. A.; Yoon, T. P. Photocatalytic reductive cyclizations of enones: Divergent reactivity of photogenerated radical and radical anion intermediates. *Chem. Sci.* **2011**, *2*, 2115-2119. (b) Du, J.; Yoon, T. P. Crossed Intermolecular [2+2] Cycloadditions of Acyclic Enones via Visible Light Photocatalysis. *J. Am. Chem. Soc.* **2009**, *131*, 14604-14605. (c) Ju, T.; Zhou, Y.-Q.; Cao, K.-G.; Fu, Q.; Ye, J.-H.; Sun, G.-Q.; Liu, X.-F.; Chen, L.; Liao, L.-L.; Yu, D.-G. Dicarboxylation of alkenes, allenes and (hetero)arenes with CO<sub>2</sub> via visible-light photoredox catalysis. *Nat. Catal.* **2021**, *4*, 304-311. (d) Yue, J.-P.; Xu, J.-C.; Luo, H.-T.; Chen, X.-W.; Song, H.-X.; Deng, Y.; Yuan, L.; Ye, J.-H.; Yu, D.-G. Metallaphotoredox-enabled aminocarboxylation of alkenes with CO<sub>2</sub>. *Nat. Catal.* **2023**, *6*, 959-968.

(16) Czyz, M. L.; Taylor, M. S.; Horngren, T. H.; Polyzos, A. Reductive Activation and Hydrofunctionalization of Olefins by Multiphoton Tandem Photoredox Catalysis. *ACS Catal.* **2021**, *11*, 5472-5480.

(17) Zhang, B.; Li, T.-T.; Mao, Z.-C.; Jiang, M.; Zhang, Z.; Zhao, K.; Qu, W.-Y.; Xiao, W.-J.; Chen, J.-R. Enantioselective Cyanofunctionalization of Aromatic Alkenes via Radical Anions. *J. Am. Chem. Soc.* **2024**, *146*, 1410-1422.

(18) Connell, T. U.; Fraser, C. L.; Czyz, M. L.; Smith, Z. M.; Hayne, D. J.; Doeven, E. H.; Agugiaro, J.; Wilson, D. J. D.; Adcock, J. L.; Scully, A. D.; et al. The Tandem Photoredox Catalysis Mechanism of [Ir(ppy)<sub>2</sub>(dtb-bpy)]<sup>+</sup> Enabling Access to Energy Demanding Organic Substrates. *J. Am. Chem. Soc.* **2019**, *141*, 17646-17658.

(19) (a) Grodzka, P. G.; Elving, P. J. Polarographic Reduction of the Phenyl-Substituted Ethenes: I. Relation of Postulated Mechanisms to Theoretical Behavior Patterns. *J. Electrochem. Soc.* **1963**, *110*, 225. (b) Funt, B. L.; Gray, D. G. A Study of Some Primary Processes in Electropolymerization by Cyclic Voltammetry of Phenyl-Substituted Ethylenes. *J. Electrochem. Soc.* **1970**, *117*, 1020. (c) Engels, R.; Schäfer, H. J. Cathodic Acylation of Aryl Olefins. *Angew. Chem., Int. Ed. Engl.* **1978**, *17*, 460-460. (d) Fruianu, M.; Marchetti, M.; Melloni, G.; Sanna, G.; Seeber, R.

Electrochemical reduction of 1,1-diaryl-substituted ethenes in dimethylformamide. *J. Chem. Soc. Perkin Trans. 2.* **1994**, 2039-2044.

(20) Venditto, N. J.; Liang, Y. S.; El Mokadem, R. K.; Nicewicz, D. A. Ketone–Olefin Coupling of Aliphatic and Aromatic Carbonyls Catalyzed by Excited-State Acridine Radicals. *J. Am. Chem. Soc.* **2022**, *144*, 11888-11896.

(21) MacKenzie, I. A.; Wang, L.; Onuska, N. P. R.; Williams, O. F.; Begam, K.; Moran, A. M.; Dunietz, B. D.; Nicewicz, D. A. Discovery and characterization of an acridine radical photoreductant. *Nature* **2020**, *580*, 76-80.

(22) (a) Heinze, J. Cathodic Reactions of Hydrocarbons, Olefins, and Aromatic Compounds. In *Encyclopedia of Electrochemistry*, 2007. (b) Zeng, L.; Wang, J.; Wang, D.; Yi, H.; Lei, A. Comprehensive Comparisons between Directing and Alternating Current Electrolysis in Organic Synthesis. *Angew. Chem. Int. Ed.* **2023**, *62*, e202309620.

(23) (a) Huck, C. J.; Sarlah, D. Shaping Molecular Landscapes: Recent Advances, Opportunities, and Challenges in Dearomatization. *Chem* **2020**, *6*, 1589-1603. (b) Kim, A. N.; Stoltz, B. M. Recent Advances in Homogeneous Catalysts for the Asymmetric Hydrogenation of Heteroarenes. *ACS Catal.* **2020**, *10*, 13834-13851. (c) Wiesenfeldt, M. P.; Nairoukh, Z.; Dalton, T.; Glorius, F. Selective Arene Hydrogenation for Direct Access to Saturated Carbo- and Heterocycles. *Angew. Chem. Int. Ed.* **2019**, *58*, 10460-10476. (d) Ji, P.; Meng, X.; Chen, J.; Gao, F.; Xu, H.; Wang, W. Combining photoredox catalysis and hydrogen atom transfer for dearomative functionalization of electron rich heteroarenes. *Chem. Sci.* **2023**, *14*, 3332-3337.

(24) (a) Kratena, N.; Marinic, B.; Donohoe, T. J. Recent advances in the dearomative functionalisation of heteroarenes. *Chem. Sci.* **2022**, *13*, 14213-14225. (b) Roche, S. P.; Porco Jr., J. A. Dearomatization Strategies in the Synthesis of Complex Natural Products. *Angew. Chem. Int. Ed.* **2011**, *50*, 4068-4093. (c) Zheng, C.; You, S.-L. Advances in Catalytic Asymmetric Dearomatization. *ACS Cent. Sci.* **2021**, *7*, 432-444. (d) Ji, P.; Duan, K.; Li, M.; Wang, Z.; Meng, X.; Zhang, Y.; Wang, W. Photochemical dearomative skeletal modifications of heteroaromatics. *Chem. Soc. Rev.* **2024**, Advance Article.

(25) Wallentin, C.-J.; Nguyen, J. D.; Finkbeiner, P.; Stephenson, C. R. J. Visible Light-Mediated Atom Transfer Radical Addition via Oxidative and Reductive Quenching of Photocatalysts. *J. Am. Chem. Soc.* **2012**, *134*, 8875-8884.

(26) (a) Qin, X.; Lee, M. W. Y.; Zhou, J. S. Nickel-Catalyzed Asymmetric Reductive Heck Cyclization of Aryl Halides to Afford Indolines. *Angew. Chem. Int. Ed.* **2017**, *56*, 12723-12726. (b) Zhou, W.-J.; Wang, Z.-H.; Liao, L.-L.; Jiang, Y.-X.; Cao, K.-G.; Ju, T.; Li, Y.; Cao, G.-M.; Yu, D.-G. Reductive dearomative arylcarboxylation of indoles with CO<sub>2</sub> via visible-light photoredox catalysis. *Nat. Commun.* **2020**, *11*, 3263.

(27) (a) Varlet, T.; Bouchet, D.; Van Elslande, E.; Masson, G. Decatungstate-Photocatalyzed Dearomative Hydroacylation of Indoles: Direct Synthesis of 2-Acylindolines. *Chem. Eur. J.* **2022**, *28*, e202201707. (b) Zhang, Y.; Ji, P.; Gao, F.; Huang, H.; Zeng, F.; Wang, W. Photoredox Asymmetric Nucleophilic Dearomatization of Indoles with Neutral Radicals. *ACS Catal.* **2021**, *11*, 998-1007. (c) Zhang, Y.; Ji, P.; Gao, F.; Dong, Y.; Huang, H.; Wang, C.; Zhou, Z.; Wang, W. Organophotocatalytic dearomatization of indoles, pyrroles and benzo(thio)furans via a Giese-type transformation. *Commun. Chem.* **2021**, *4*, 20. (d) Montinho-Inacio, E.; Bouchet, D.; Ma, W. Y.; Retailleau, P.; Neuville, L.; Masson, G. Decatungstate-Photocatalyzed Diastereoselective Dearomative Hydroalkylation of Indoles. *Eur. J. Org. Chem.* **2024**, e202400248.

(28) Di, J.; He, H.; Wang, F.; Xue, F.; Liu, X.-Y.; Qin, Y. Regiospecific alkyl addition of (hetero)arene-fused thiophenes enabled by a visible-light-mediated photocatalytic desulfuration approach. *Chem. Commun.* **2018**, *54*, 4692-4695.

(29) (a) Mikhael, M.; Alektiar, S. N.; Yeung, C. S.; Wickens, Z. K. Translating Planar Heterocycles into Three-Dimensional Analogs by Photoinduced Hydrocarboxylation\*\*. *Angew. Chem. Int. Ed.* **2023**, *62*, e202303264. (b) Edgecomb, J. M.; Alektiar, S. N.; Cowper, N. G. W.; Sowin, J. A.; Wickens, Z. K. Ketyl Radical Coupling Enabled by Polycyclic Aromatic Hydrocarbon Electrophotocatalysts. *J. Am. Chem. Soc.* **2023**, *145*, 20169-20175. (c) Mangaonkar, S. R.; Hayashi, H.; Takano, H.; Kanna, W.; Maeda, S.; Mita, T. Photoredox/HAT-Catalyzed Dearomative Nucleophilic Addition of the CO<sub>2</sub> Radical Anion to (Hetero)Aromatics. *ACS Catal.* **2023**, *13*, 2482-2488.

(30) You, Y.; Kanna, W.; Takano, H.; Hayashi, H.; Maeda, S.; Mita, T. Electrochemical Dearomative Dicarboxylation of Heterocycles with Highly Negative Reduction Potentials. *J. Am. Chem. Soc.* **2022**, *144*, 3685-3695.

(31) (a) Kawamata, Y.; Hayashi, K.; Carlson, E.; Shaji, S.; Waldmann, D.; Simmons, B. J.; Edwards, J. T.; Zapf, C. W.; Saito, M.; Baran, P. S. Chemoselective Electrosynthesis Using Rapid Alternating Polarity. *J. Am. Chem. Soc.* **2021**, *143*, 16580-16588. (b) Hayashi, K.; Griffin, J.; Harper, K. C.; Kawamata, Y.; Baran, P. S. Chemoselective (Hetero)Arene Electroreduction Enabled by Rapid Alternating Polarity. *J. Am. Chem. Soc.* **2022**, *144*, 5762-5768.

(32) (a) Blanco, D. E.; Lee, B.; Modestino, M. A. Optimizing organic electrosynthesis through controlled voltage dosing and artificial intelligence. *Proc. Natl. Acad. Sci. U.S.A.* **2019**, *116*, 17683-17689. (b) Boudjelel, M.; Zhong, J.; Ballerini, L.; Vanswearingen, I.; Al-Dhufari, R.; Malapit, C. Electrochemical generation of aryl radicals from organoboron reagents enabled by pulsed electrosynthesis. *Angew. Chem. Int. Ed.* **2024**, e202406203.

(33) Bortnikov, E. O.; Smith, B. S.; Volochnyuk, D. M.; Semenov, S. N. Stirring-Free Scalable Electrosynthesis Enabled by Alternating Current. *Chem. Eur. J.* **2023**, *29*, e202203825.

(34) Li, P.; Jiao, Y.; Huang, J.; Chen, S. Electric Double Layer Effects in Electrocatalysis: Insights from Ab Initio Simulation and Hierarchical Continuum Modeling. *JACS Au* **2023**, *3*, 2640-2659.

(35) (a) Carabajal, M. P. A.; Piloto-Ferrer, J.; Nicollela, H. D.; Squarisi, I. S.; Prado Guissone, A. P.; Esperandim, T. R.; Tavares, D. C.; Isla, M. I.; Zampini, I. C. Antigenotoxic, antiproliferative and antimetastatic properties of a combination of native medicinal plants from Argentina. *J. Ethnopharmacol.* **2021**, *267*, 113479. (b) Iwadate, T.; Nihei,

K.-i. Chemical synthesis, redox transformation, and identification of sonnerphenolic C, an antioxidant in *Acer nikoense*. *Biorg. Med. Chem. Lett.* **2017**, *27*, 1799-1802. (c) Yoon, J.; Choi, H.; Lee, H. J.; Ryu, C. H.; Park, H.-g.; Suh, Y.-g.; Oh, U.; Jeong, Y. S.; Choi, J. K.; Park, Y.-H.; et al. Chain-Branched acyclic phenethylthiocarbamates as vanilloid receptor antagonists. *Biorg. Med. Chem. Lett.* **2003**, *13*, 1549-1552.

(36) Francisco, K. R.; Monti, L.; Yang, W.; Park, H.; Liu, L. J.; Watkins, K.; Amarasinghe, D. K.; Nalli, M.; Roberto Polaquini, C.; Regasini, L. O.; et al. Structure-activity relationship of dibenzylideneacetone analogs against the neglected disease pathogen, *Trypanosoma brucei*. *Biorg. Med. Chem. Lett.* **2023**, *81*, 129123.

(37) Fujiwara, M.; Yagi, N.; Miyazawa, M. Acetylcholinesterase Inhibitory Activity of Volatile Oil from *Peltophorum dasyrachis* Kurz ex Bakar (Yellow Batai) and Bisabolane-Type Sesquiterpenoids. *J. Agric. Food. Chem.* **2010**, *58*, 2824-2829.

(38) (a) Dong, Z.; MacMillan, D. W. C. Metallaphotoredox-enabled deoxygenative arylation of alcohols. *Nature* **2021**, *598*, 451-456. (b) Li, Z.; Sun, W.; Wang, X.; Li, L.; Zhang, Y.; Li, C. Electrochemically Enabled, Nickel-Catalyzed Dehydroxylative Cross-Coupling of Alcohols with Aryl Halides. *J. Am. Chem. Soc.* **2021**, *143*, 3536-3543. (c) Lin, Q.; Ma, G.; Gong, H. Ni-Catalyzed Formal Cross-Electrophile Coupling of Alcohols with Aryl Halides. *ACS Catal.* **2021**, *11*, 14102-14109. (d) Chi, B. K.; Widness, J. K.; Gilbert, M. M.; Salgueiro, D. C.; Garcia, K. J.; Weix, D. J. In-Situ Bromination Enables Formal Cross-Electrophile Coupling of Alcohols with Aryl and Alkenyl Halides. *ACS Catal.* **2022**, *12*, 580-586. (e) Oestreich, M.; Klare, H. F. T.; Wolff, B. Deoxygenative Cross-Coupling of Benzyl Alcohols and Boronic Acids Enabled by Transient Isoarea Formation. *Synfacts* **2022**, *18*, 1105. (f) Oestreich, M.; Klare, H. F. T.; Pommerening, P. Deoxygenative Cross-Coupling Reactions of Phenols Enabled by Transient O-Phenyl-Uronium Formation. *Synfacts* **2022**, *18*, 1108. (g) Lyon, W. L.; MacMillan, D. W. C. Expedient Access to Underexplored Chemical Space: Deoxygenative C(sp<sup>3</sup>)-C(sp<sup>3</sup>) Cross-Coupling. *J. Am. Chem. Soc.* **2023**, *145*, 7736-7742. (h) Cook, A.; St. Onge, P.; Newman, S. G. Deoxygenative Suzuki-Miyaura arylation of tertiary alcohols through silyl ethers. *Nature Synthesis* **2023**, *2*, 663-669. (i) Zhang, L.-L.; Gao, Y.-Z.; Cai, S.-H.; Yu, H.; Shen, S.-J.; Ping, Q.; Yang, Z.-P. Ni-catalyzed enantioconvergent deoxygenative reductive cross-coupling of unactivated alkyl alcohols and aryl bromides. *Nat. Commun.* **2024**, *15*, 2733. (j) Chen, R.; Intermaggio, N. E.; Xie, J.; Rossi-Ashton, J. A.; Gould, C. A.; Martin, R. T.; Alcázar, J.; MacMillan, D. W. C. Alcohol-alcohol cross-coupling enabled by S<sub>H</sub>2 radical sorting. *Science* **2024**, *383*, 1350-1357. (k) Carson, W. P., II; Tsymbal, A. V.; Pipal, R. W.; Edwards, G. A.; Martinelli, J. R.; Cabré, A.; MacMillan, D. W. C. Free-Radical Deoxygenative Amination of Alcohols via Copper Metallaphotoredox Catalysis. *J. Am. Chem. Soc.* **2024**,

(39) Kim, Y.; Park, G. D.; Balamurugan, M.; Seo, J.; Min, B. K.; Nam, K. T. Electrochemical  $\beta$ -Selective Hydrocarboxylation of Styrene Using CO<sub>2</sub> and Water. *Adv. Sci.* **2020**, *7*, 1900137.

(40) Hu, P.; Peters, B. K.; Malapit, C. A.; Vantourout, J. C.; Wang, P.; Li, J.; Mele, L.; Echeverria, P.-G.; Minter, S. D.; Baran, P. S. Electroreductive Olefin-Ketone Coupling. *J. Am. Chem. Soc.* **2020**, *142*, 20979-20986.

(41) Savéant, J.-M. C., C. *Elements of Molecular and Biomolecular Electrochemistry: An Electrochemical Approach to Electron Transfer Chemistry*; John Wiley & Sons Inc., 2019.

(42) (a) Harris, P. J. F. Fullerene-related structure of commercial glassy carbons. *Philos. Mag.* **2004**, *84*, 3159-3167. (b) Romero, N. A.; Nicewicz, D. A. Mechanistic Insight into the Photoredox Catalysis of Anti-Markovnikov Alkene Hydrofunctionalization Reactions. *J. Am. Chem. Soc.* **2014**, *136*, 17024-17035.

(43) Molina, A.; González, J.; Laborda, E.; Compton, R. G. Analytical solutions for fast and straightforward study of the effect of the electrode geometry in transient and steady state voltammeteries: Single- and multi-electron transfers, coupled chemical reactions and electrode kinetics. *J. Electroanal. Chem.* **2015**, *756*, 1-21.

(44) (a) Mirčeski, V.; Lovrić, M. Split square-wave voltammograms of surface redox reactions. *Electroanalysis* **1997**, *9*, 1283-1287. (b) Mirceski, V.; Gulaboski, R.; Lovric, M.; Bogeski, I.; Kappl, R.; Hoth, M. Square-Wave Voltammetry: A Review on the Recent Progress. *Electroanalysis* **2013**, *25*, 2411-2422. (c) Gulaboski, R. Surface ECE mechanism in protein film voltammetry—a theoretical study under conditions of square-wave voltammetry. *J. Solid State Electrochem.* **2009**, *13*, 1015-1024.

(45) Zhang, B.; Li, T.-T.; Mao, Z.-C.; Jiang, M.; Zhang, Z.; Zhao, K.; Qu, W.-Y.; Xiao, W.-J.; Chen, J.-R. Enantioselective Cyanofunctionalization of Aromatic Alkenes via Radical Anions. *J. Am. Chem. Soc.* **2024**, *146*, 1410-1422.

(46) Czyn, M.; Horngren, T.; Kondopoulos, A.; Franov, L.; Forni, J.; Pham, L. N.; Coote, M.; Polyzos, A. Photocatalytic Generation of Alkyl Carbanions from Alkenes. *ChemRxiv* **2023**, doi:10.26434/chemrxiv-22023-qrkjs.